Magnetic order in a submicron patterned permalloy film studied by resonant x-ray scattering

Carlo Spezzani,[1] Mauro Fabrizioli,[2] Patrizio Candeloro,[2] Enzo Di Fabrizio,[2] Giancarlo Panaccione,[2] and Maurizio Sacchi[1]
[1]*Laboratoire pour l'Utilisation du Rayonnement Electromagnétique (LURE), Centre Universitaire Paris-Sud, B.P. 34, 91898 Orsay, France*
[2]*Istituto Nazionale per la Fisica della Materia, INFM, Laboratorio TASC, S.S. 14, Km 163.5, AREA Science Park, 34012 Basovizza, Trieste, Italy*
(Received 14 December 2003; revised manuscript received 21 April 2004; published 25 June 2004)

We have used specular and off-specular x-ray scattering to follow the field dependent magnetization in an array of 1000 nm$\times$350 nm permalloy rectangles. Sensitivity to the magnetic properties of the permalloy was obtained by tuning the x-ray energy to the Fe 2*p* resonance. The corresponding wavelength matches the Bragg condition for the regular horizontal structure of the pattern. The magnetic behavior was found to depend on the orientation of the field with respect to the rectangles: we observed the presence of a strong magnetic anisotropy induced by the patterning, with a magnetic hard axis in the direction of the shorter side of the rectangles.

DOI: 10.1103/PhysRevB.69.224412 PACS number(s): 75.75.+a, 78.70.Ck, 78.20.Ls

I. INTRODUCTION

Submicron sized structures are currently attracting attention especially where there is a potential for applications in the fields of magnetic storage media and solid-state devices. An understanding of the magnetic-field-dependent correlations within an array of submicrometric objects is important both fundamentally and practically. Static[1–3] and dynamic[4–6] magnetic properties in microstructured elements have been investigated by several groups recently, using various complementary approaches that have brought to light important effects such as spin-wave quantization and dipolar coupling between dots. Direct imaging of patterned magnetic structures was obtained by microscopy techniques, showing that the magnetic response to applied fields strongly depends on the size and aspect ratio of the dots.[7]

In this paper we report on the analysis of a matrix of rectangular dots of permalloy ($Ni_{81}Fe_{19}$) measuring 1000 nm$\times$350 nm with a thickness of 25 nm. We have used resonant scattering of polarized soft x rays to investigate their magnetic behavior as a function of the applied field. This technique couples the advantages of structural analysis to sensitivity to electronic structure. The former is inherent to x-ray scattering, the latter the consequence of a spectroscopic response to resonant core-electron excitations where optical constants depend on the local magnetic moment of the scattering ion.[8] In a magnetic structure with an appropriate order parameter, one can match Bragg's law at a photon energy that resonantly excites an inner shell electron, simultaneously probing structural and magnetic properties, element selectively.[9–13] Magnetic contributions to the scattering amplitude are enhanced when the electron excitation directly involves those orbitals that define the magnetic properties of the absorbing ion, as is the case for the 2*p* to 3*d* excitations in 3*d* transition metals.

When a sample has lateral periodicity, as here, it is possible to perform off-specular scattering measurements, tuning the in-plane component of the momentum transfer to the structural[14,15] or magnetic[16,17] order parameter. We have used this approach to investigate the existence of a correlation in the magnetic properties of the dots within the array.

II. EXPERIMENTAL DETAILS

A. Sample preparation

The patterned magnetic sample was prepared at the LILIT beamline (ELETTRA, Trieste), using x-ray lithography in combination with a lift-off process. First an x-ray mask was prepared using electrolytic growth and electron beam lithography. The absorption contrast of the mask was obtained by forming an Au pattern on a Cr–Au base plating deposited on a highly transparent 100 nm thick silicon nitride (Si_3N_4) membrane.[18,19] The sample was prepared on a silicon substrate coated with 450 nm of resist (PMMA). First it was exposed through the mask to a 1.5 keV x-ray beam, receiving a total dose of 5000 mJ/cm^2. After the exposure, the resist was developed in MIBK:IPA=1:3 solution at room temperature for 15 s and rinsed in IPA. Residual resist in the exposed regions was removed by oxygen plasma reactive ion etching. On top of the patterned resist, we deposited 25 nm of permalloy followed by 2 nm of germanium as a protective layer. The remaining resist was removed by a lift-off process in a warm acetone bath, releasing the isolated magnetic rectangles. Figure 1 shows a scanning electron microscope (SEM) image of the patterned permalloy sample. The rectangles are 1000 nm$\times$350 nm and spaced 250 nm apart lengthwise and 200 nm apart in the direction of the shorter side. This gives rise to two order parameters: 1250 nm and 550 nm, respectively. Typically, the dimensions of the rectangles are precise to within 20–30 nm. The array extends over a total area of 1×1 mm^2. The patterned area is framed by a continuous permalloy film, also 25 nm thick.

B. X-ray scattering measurements

Measurements were performed at the Advanced Light Source synchrotron radiation facility (Berkeley), using the

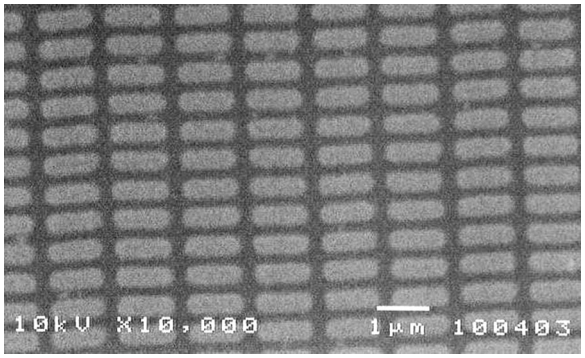

FIG. 1. SEM image of the patterned permalloy film.

reflectometer endstation of the x-ray metrology beamline 6.3.2 (Center for X-Ray Optics[20]). Details of the experimental set up were the same as reported in previous publications.[12,13] A flux of $\sim 10^9$ photons per second with a resolving power of 2000 was available at the Fe $L_{2,3}$ edges (700–730 eV), with a circular polarization rate of 60%. A sketch of the experimental geometry is given in Fig. 2: we will identify the *z* axis as the normal to the sample surface (*xy* plane), and *xz* as the incidence plane (containing the incoming photon momentum and the sample normal). The scattering geometry was coplanar, i.e., the scattering plane coincided with the incidence *xz* plane.

The beam size at the sample position was about 300 μm horizontal by 100 μm vertical. The latter is the 1:1 image of the monochromator exit slit obtained via a bendable mirror. Therefore, in principle, the photon spot could be placed entirely onto the patterned area for a sample angle θ_S greater than 6°. As we will see below, this is an optimistic assumption. We performed most of our measurements by placing the detector angle θ_D at 18°, where we found a good compromise between beam imprint on the sample, scattered intensity and magnetic signal intensity. An external magnetic field, up to about 1 kOe, could be applied using a small electromagnet placed behind the sample surface. As depicted in Fig. 2, the field was oriented in the sample surface, either parallel (*x* axis, longitudinal geometry) or perpendicular (*y* axis, transverse geometry) to the scattering plane.

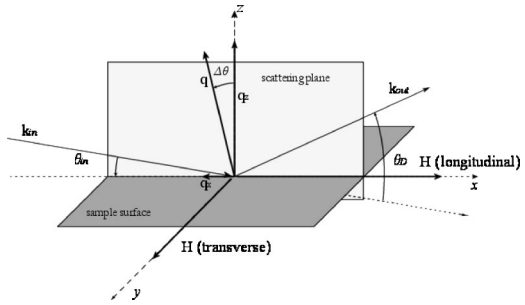

FIG. 2. Sketch of the x-ray scattering set up (see text). The experiment was performed in coplanar geometry, applying the magnetic field either parallel (longitudinal geometry) or perpendicular (transverse geometry) to the scattering plane.

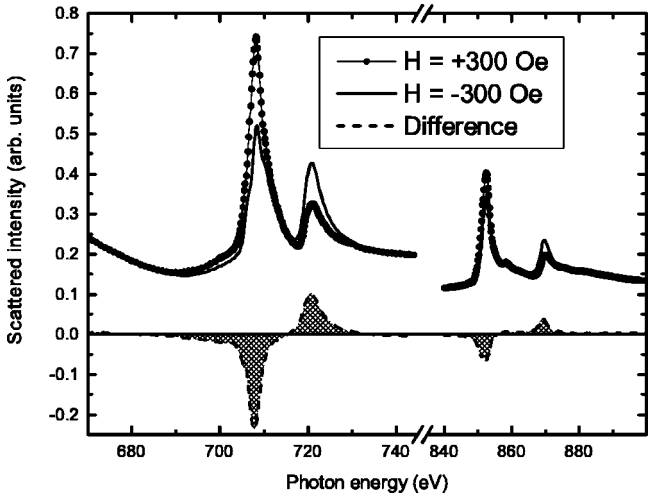

FIG. 3. Specular reflectivity (θ=9°) of elliptically polarized x rays as a function of their energy over the range including the 2*p* resonances of Fe and Ni. A field of 300 Oe (positive and negative) is applied along the *x* axis. The difference observed for opposite orientations of the field is shown as a dashed line.

III. RESULTS AND DISCUSSION

A. Energy and angular dependence of the diffuse scattering

Figure 3 shows an example of energy dependent specular reflectivity measured for two opposite values of the applied field (H = ±300 Oe, longitudinal geometry). The energy range covers both the Fe 2*p* (700–730 eV) and Ni 2*p* (850–880 eV) resonances. The corresponding magnetic signal (difference between the two curves for opposite magnetizations) is given by the dashed line at the bottom. The field dependent resonant scattering measurements at fixed photon energy that we will discuss in Sec. III B were taken at 707.5 eV, corresponding to the Fe, L_3 edge region.

Figure 4 shows the result of a θ_S scan at fixed θ_D=12.5°

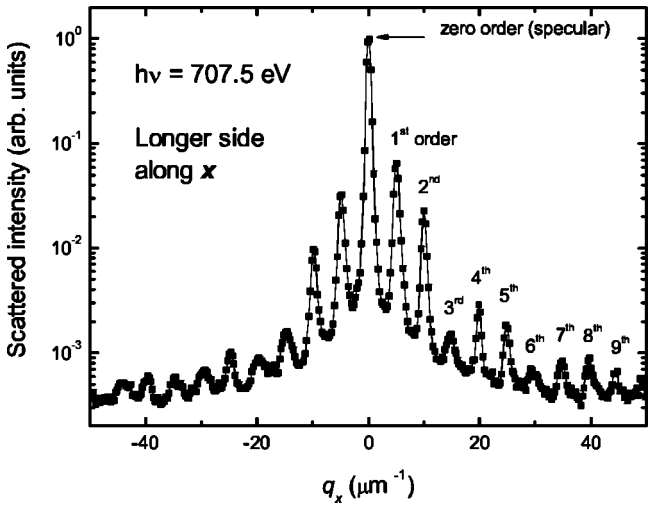

FIG. 4. Diffuse intensity versus q_x (rocking scan, see text). Rectangles are aligned with their longer side parallel to the scattering plane. The position of the first order peak corresponds to $d = 2\pi/q_x = 1.247$ μm.

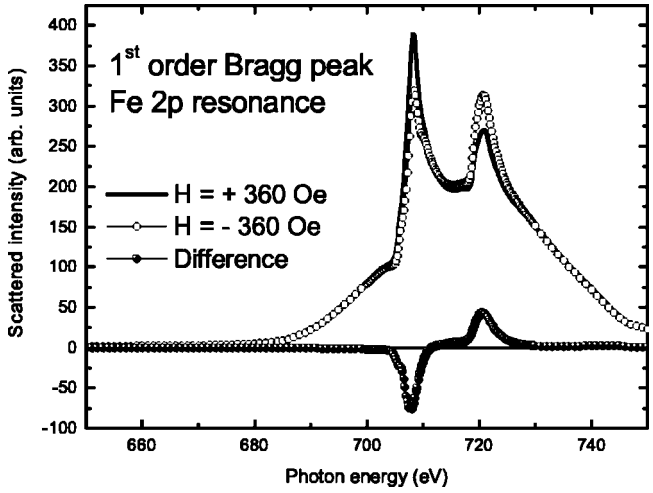

FIG. 5. Scattered intensity versus photon energy across the Fe $2p$ resonance. Conditions are as in Fig. 3, but with $q_x=2\pi/d$ ($n=1$) instead of $q_x=0$.

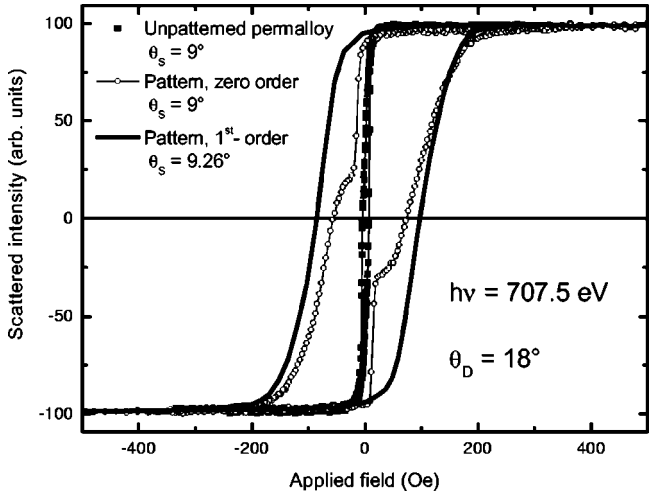

FIG. 6. Scattered intensity as a function of the applied field at the Fe $2p$ resonance. The intensity has been arbitrarily rescaled between −100 and +100 for each curve. Squares: specular reflectivity from the continuous permalloy film framing the patterned area. Open circles: specular reflectivity (zero order) from the patterned area. Line: first order scattering from the patterned area.

(rocking scan), with the long side of the rectangles oriented along x. The intensity is plotted versus q_x, the component parallel to the surface of the momentum transfer vector $\mathbf{q}=\mathbf{k}_{\text{out}}-\mathbf{k}_{\text{in}}$, where $\mathbf{k}_{\text{in,out}}$ are the wave vectors of the incoming and outgoing photons of wavelength λ (see Fig. 2). Defining $\theta=\theta_D/2$ and $\Delta\theta=\theta_S-\theta$, we have

$$q=|\mathbf{k}_{\text{out}}-\mathbf{k}_{\text{in}}|=\frac{4\pi}{\lambda}\sin(\theta),$$

$$q_x=q\,\sin(\Delta\theta)=\frac{4\pi}{\lambda}\sin(\theta)\sin(\Delta\theta),$$

$$q_z=q\,\cos(\Delta\theta)=\frac{4\pi}{\lambda}\sin(\theta)\cos(\Delta\theta),$$

$q_x=0$ corresponds to the specular condition, or, by analogy with diffraction gratings, to the zero order position. As for a grating, nth order peaks correspond to $q_x=2n\pi/d$, where n can take positive and negative integer values and d is the order parameter in the x direction.[17,21,22] In Fig. 4, the position of the first order peak is $q_x=5.036\ \mu\text{m}^{-1}$, corresponding to $d=1.247\ \mu$m, in excellent agreement with the structural parameters given above.

Figure 5 shows the result of an energy scan analogous to that of Fig. 3, but with the sample angle set to match the first order peak of the diffuse scattering at 707.5 eV. The shape of the energy dependent scattered intensity is quite different from the specular reflectivity curves. In particular, the intensity variation across the edge region is much stronger (more than two orders of magnitude in Fig. 5, compared to a factor 5 in Fig. 3), reflecting the fact that, for fixed values of both θ_D and θ_S, the Bragg condition $q_x=2\pi/d$ is satisfied exactly only at one wavelength.[23] The shape of the magnetic contribution, however, is similar to that of Fig. 3.

B. Field dependent scattered intensity

Scattered intensity at fixed θ_D, θ_S, and $\hbar\omega$ (707.5 eV) was measured as a function of the applied field. Under these conditions, the variation of the scattered intensity with the applied field gives a measure, on a relative scale, of the local magnetic moment of Fe projected along the x axis (see Fig. 2). By alternately applying the external field H along x and y axes, we can probe the Fe magnetization parallel and perpendicular to H. These field dependent intensity curves can be assimilated to element specific hysteresis curves.[3] Figure 6 compares three examples of such measurements ($\theta_D=18°$), with the long side of the rectangles and the applied field both oriented along x. The intensities have been arbitrarily rescaled between −100 and +100 for each curve.

Squares are the result of a specular reflectivity measurement ($\theta_S=9°$) on the continuous permalloy film framing the patterned area. The measured coercive field H_c is 5 ± 1 Oe and remanence is in the order of 60%. These values are typical of a thin permalloy film.

Open circles in Fig. 6 represent specular reflectivity from the patterned area (zero order scattering, $q_x=0$), giving the average magnetization of Fe over the illuminated area. Remanence in this case is close to unity, but two components can be clearly identified in the hysteresis curve. We have modeled this and other similar curves by summing two square loops of adjustable width and height, in order to estimate the coercive field and the relative importance of each component. The narrow loop represents roughly 30% of the total intensity variation as a function of H and its coercive field is $H_c=11\pm3$ Oe. The second loop has a larger H_c of about 90 ± 10 Oe.

Finally, the continuous line was obtained by matching the first order peak ($\theta_S=9.26°$, $q_x=5.04\ \mu\text{m}^{-1}$), with the long side of the rectangles oriented along x. The hysteresis curve displays a single loop with almost complete remanence (95%) and a coercive field of 90 ± 3 Oe.

By comparing these curves, we can easily identify the hysteresis on the first order scattering peak with the broader component measured at zero order. The sides of the hysteresis loop are rather slanted, with a large difference between coercive (90 Oe) and saturation (250 Oe) fields. Therefore, the magnetization rotation does not take place as an abrupt switching as a function of field, but is characterized by intermediate magnetic configurations. The hysteresis loop is measured at the first order scattering peak, which means that these configurations repeat themselves in a regular way throughout the pattern and must be related to the specific shape of the rectangles. The edges of the dots act as pinning centers for magnetization reversal, determining an increased coercive field with respect to the continuous film. Moreover, magnetic poles are likely to form at the edges of the rectangles, particularly at the corners. The demagnetizing field associated to these poles can be large enough to be responsible for the slanted sides of the hysteresis loop, indicating the difficulty of reaching saturation in the patterned area compared to the continuous film. As mentioned in the Introduction, remanent magnetization in permalloy rectangles was shown to vary strongly with size and aspect ratio. Gomez *et al.*[7] reported the formation of several types of complex magnetic structures in zero field, depending on the shape of the rectangles and on the external field direction. The high remanence (95%) that we observe after saturation implies that, in our sample, the zero field state is characterized by a rather homogeneous magnetization within each dot, excluding the formation of closure domain patterns.

The hysteresis curve at zero order measures the field dependence of the average Fe magnetization over the entire illuminated area, while at first order the hysteresis measures only those changes that repeat regularly over the pattern. The presence of a narrow component in the zero order, but not in first order, hysteresis curve (Fig. 6) indicates that part of the illuminated sample behaves like the unpatterned film. We conclude that, although the sample angle was set at 9°, the zero order measurement is affected by some of the photon beam spilling over the continuous permalloy film framing the pattern. One result that comes out clearly from Fig. 6 is that, by choosing to work at the first order Bragg peak, we automatically exclude all contributions that do not come from the regular pattern, cleaning up the signal from spurious sources.

We have performed analogous measurements aligning the rectangles with their short side in the scattering plane. The rocking scan in Fig. 7 gives the first order peak at $q_x = 11.897\ \mu\text{m}^{-1}$, corresponding to a horizontal order parameter of 530 nm, to be compared to the nominal 550 nm of the pattern design.

The appearance of weak structures right in between Bragg peaks of the grating deserves some comments. We have verified, by introducing appropriate filters in the beam path, that they originate from second order light from the monochromator, i.e., in this case, a contamination at 1415 eV photon energy. This implies that, calculating q_x for 707.5 eV, they appear at half of the correct value.[24]

A different magnetic response is expected when the field is applied along one side or the other of the rectangles because they are highly asymmetric. Figure 8 compares two

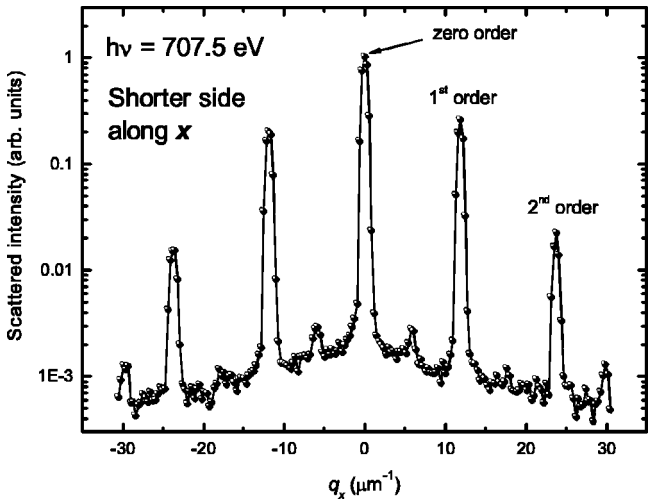

FIG. 7. Rocking scan as in Fig. 4. Rectangles are aligned with their shorter side parallel to the scattering plane. The position of the first order peak corresponds to an order parameter $d = 2\pi/q_x = 0.53\ \mu$m.

hysteresis curves, both at the first order Bragg peak, obtained with the field aligned along the major and minor sides of the rectangles. The short side behaves as a hard axis for the sample magnetization, and we were not able to reach magnetic saturation in this direction with a field of up to 800 Oe (therefore remanence could not be evaluated from our measurements). A small hysteresis loop is observed over the range ±100 Oe.

Working at the first order Bragg peak, we probe the presence of magnetic structures that repeat themselves in every rectangle. By varying q_x, we can pick up other correlation lengths within the array. A way of probing correlations between pairs of rectangles, for instance, is to set q_x at half the value of the first order peak

$$q_x = \tfrac{1}{2}(2\pi/d) = \pi/d = 2\pi/d'; \quad d' = 2d.$$

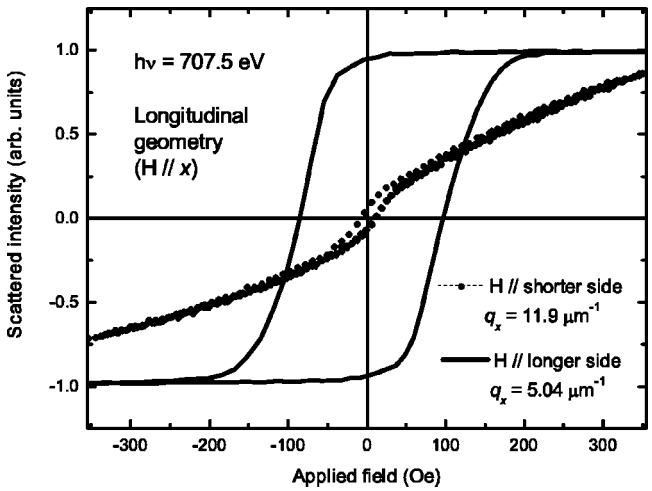

FIG. 8. Field dependent scattering at the first order peak with the field applied along the *x* axis. Line: longer side along *x* (same as in Fig. 6). Dots: shorter side along *x*.

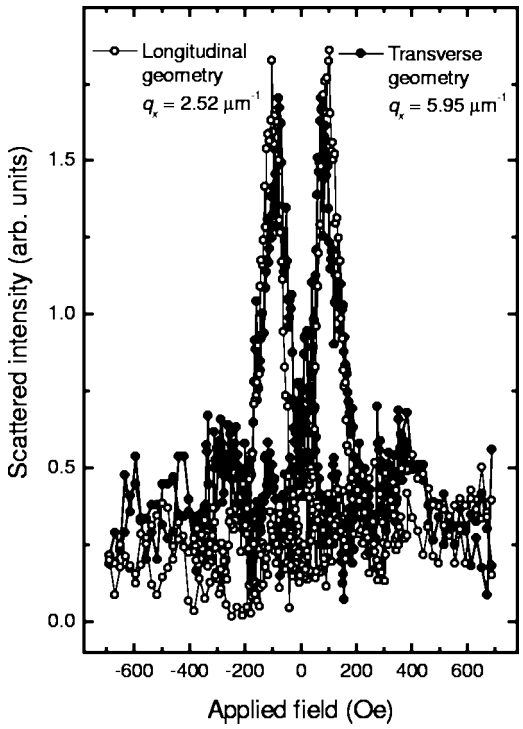

FIG. 9. Intensity scattered at the half order position as a function of the field applied along the easy magnetization axis (longer side of the rectangles). Open circles: longitudinal geometry ($H \| x$). Filled circles: transverse geometry ($H \perp x$). $\hbar\omega = 707.5$ eV.

This corresponds to introducing a new order parameter $d' = 2d$, or, as often said, to taking $n = \frac{1}{2}$ in the equation $q_x = 2n\pi/d$ (half order position with respect to the order parameter d). In Fig. 9 we compare hysteresis curves obtained by measuring the intensity scattered at the half order position, with the field applied along the major axis of the rectangles, in both longitudinal (open circles) and transverse (filled circles) geometries (see Fig. 2). The two curves are very similar, especially if one considers that the scale of the intensities (although in arbitrary units) is the same for both. A strong enhancement (4–6-fold) of the measured signal is observed at ±100 Oe, the sign depending on the direction of the field variation. Outside the ±200 Oe region, the scattered intensity is extremely weak and displays no field dependence, confirming the purely magnetic origin of the peaks. The scattered intensity peaks around 80–100 Oe, i.e., around the coercive field of the hysteresis loop for the long side of the rectangles. This field dependence compares very well to the derivative of the hysteresis curve at the first order peak shown in Fig. 6.

It is worth remembering that the presence of contamination in the x-ray beam from second order light[24] introduces, at most, a constant background in the field dependent measurements, since the scattering amplitude of 1415 eV photons is insensitive to the magnetization state of Fe.

As mentioned above, at the half order position we are probing correlations over a distance that is double the period of the pattern, i.e., a periodic structure that implies pairs of rectangles. Extra intensity at this angular position may come from the systematic antiparallel coupling of the magnetization in neighboring rectangles, giving rise to a magnetic structure of double order parameter. Hysteresis curves similar to those in Fig. 9 have been observed, for instance, in magnetoresistive multilayers displaying antiferromagnetic (AF) alignment of neighboring ferromagnetic sheets,[12,13,25] and in laterally ordered stripes.[16,17]

We want to point out, though, that these magnetic signals are rather weak compared to the field dependence observed at the first order peak. Moreover, we observe the same intensity in longitudinal and transverse geometries, while the latter should give a relatively stronger contribution in case of induced AF coupling at the coercive field.[25,26] Finally, the effect can be observed, with varying intensity, over a fairly large range of q_x values, indicating that the order repeats over a limited number of periods only.

From these observations we conclude that the scattered intensity at the half order position is indicative of a high probability that an antiparallel coupling sets up between neighboring rectangles. This coupling can extend to several pairs, locally giving rise to an ordered magnetic structure, but the order never extends to the entire array. The same behavior is observed in both directions parallel and perpendicular to the applied field, with almost identical intensity. The magnetic superstructure can be related to a transient phase that sets up when the external field approaches H_c, determining an overall vanishing magnetization. Therefore, our results imply that the zero average magnetization is obtained with a certain degree of antiparallel alignment between the magnetization in one rectangle and in its neighbors, and that this alignment repeats itself in an ordered manner over a limited extent of the pattern.

IV. CONCLUSIONS

We have used resonant scattering of polarized soft x-rays to analyze the field dependence of the magnetization in an array of submicrometric rectangles patterned into a 25 nm thick permalloy film. Sensitivity of x-ray scattering to magnetization was obtained by using elliptically polarized light and by tuning the photon energy at the Fe $2p$ resonance.

As for a diffraction grating, the lateral modulation of the pattern produces sharp peaks in the diffuse scattering that we used to single out contributions coming from a regular magnetic structure. This allowed us to filter out other contributions from, e.g., unpatterned areas and/or nonregular patches, while illuminating and measuring the entire sample. The hysteresis curves obtained at the first order scattering peak measure the collective magnetization rotation in the array. When the field is applied along the long side of the rectangles, the hysteresis is characterized by almost complete remanence and by a coercive field H_c of 90 Oe. On the other hand, the short side is a hard axis for the magnetization of the rectangles: a very small hysteresis loop was observed and saturation could not be reached at the maximum field available in our experiment.

We have measured also the intensity scattered at the half-order position, corresponding to an order parameter that involves pairs of rectangles. We have shown that this scattering channel is of purely magnetic origin, since its intensity can

be made negligible as a function of the applied field. In the hysteresis curve (Fig. 9), the scattered intensity sharply peaks around the coercive field value, indicating that a high degree of antiparallel alignment between neighboring rectangles is reached only at H_c. As in the case of specular scattering from magnetoresistive multilayers, antiparallel magnetic coupling appears as extra intensity in the half-order scattering channel.[10] From the field and angular dependence, though, we conclude that the antiparallel alignment is rather a local property that does not extend in a regular way throughout the entire array.

Finally, our experiment also points to the interest of using soft x-ray resonant scattering for the analysis of arrays of submicrometric particles. Resonant scattering analyzes in reciprocal space a collection of objects, offering a complementary approach with respect to microscopy techniques that deal more directly with single objects in real space. Both x-ray (photoemission microscopy, see Ref. 27) and electron (Lorentz microscopy, see Ref. 7) based techniques have been used in the past to image the remanent magnetic properties of permalloy dots. The importance of combining microscopy and scattering techniques for the analysis of magnetic structures was recently pointed out in a study of the formation of magnetic domains in multilayers.[28] The combination in a single technique of structural and magnetic sensitivity together with element selectivity makes resonant scattering a remarkable tool in this field. Also, its photon-in/photon-out character makes it possible to work in the presence of time dependent magnetic fields, opening new opportunities in the investigation of collective dynamics in magnetic microstructures.

Another technique that offers similar capabilities is the diffracted magneto-optic Kerr effect performed with visible light [D-MOKE (Ref. 29)]. Strict analogies can be found even in the theoretical description of the two measurements. Apart from adding element selectivity (intrinsic to resonant x-ray spectroscopies), working with x rays implies that shorter wavelengths are employed which means that it is possible to investigate shorter lateral periods. Moreover, soft x-ray wavelengths ideally match the vertical period of typical multilayer structures. Patterning multilayers in general and magneto-resistive multilayers in particular is interesting for applications.[30] Magnetoresistive multilayers display distinct vertical order parameters for ferromagnetic and antiferromagnetic coupling.[10–13] Therefore, a peculiar feature of resonant x-ray scattering is that it makes it possible to match simultaneously lateral and vertical periods of a patterned multilayer, probing correlated magnetic order in both directions.

ACKNOWLEDGMENTS

The authors thank the staff of the Center for X-Ray Optics and of the Advanced Light Source for their efficient support, in particular Eric Gullikson for assistance at the beamline. M.S. thanks Coryn Hague for helpful discussions. This work has received the financial support of the European Community under Contract No. HPRI CT 2001 50032.

[1] M. Natali, I. L. Prejbeanu, A. Lebib, L. D. Buda, K. Ounadjela, and Y. Chen, Phys. Rev. Lett. **88**, 157203 (2002).
[2] P. Vavassori, M. Grimsditch, V. Novosad, V. Metlushko, and B. Ilic, Phys. Rev. B **67**, 134429 (2003).
[3] D. R. Lee, Y. Choi, C.-Y. You, J. C. Lang, D. Haskel, G. Srajer, V. Metlushko, B. Ilic, and S. D. Bader, Appl. Phys. Lett. **81**, 4997 (2002).
[4] J. Jorzick, S. O. Demokritov, B. Hillebrands, M. Bailleul, C. Fermon, K. Y. Guslienko, A. N. Slavin, D. V. Berkov, and N. L. Gorn, Phys. Rev. Lett. **88**, 047204 (2002).
[5] K. Y. Guslienko, R. W. Chantrell, and A. N. Slavin, Phys. Rev. B **68**, 024422 (2003).
[6] M. Bailleul, D. Olligs, and C. Fermon, Phys. Rev. Lett. **91**, 137204 (2003).
[7] R. D. Gomez, T. V. Luu, A. O. Pak, K. J. Kirk, and J. N. Chapman, J. Appl. Phys. **85**, 6163 (1999).
[8] J. P. Hannon, G. T. Trammell, M. Blume, and D. Gibbs, Phys. Rev. Lett. **61**, 1245 (1988); N. Mainkar, D. A. Browne, and J. Callaway, Phys. Rev. B **53**, 3692 (1996).
[9] D. Gibbs, D. R. Harshman, E. D. Isaacs, D. B. McWhan, D. Mills, and C. Vettier, Phys. Rev. Lett. **61**, 1241 (1988).
[10] J. M. Tonnerre, L. Sève, D. Raoux, G. Soullié, B. Rodmacq, and P. Wolfers, Phys. Rev. Lett. **75**, 740 (1995).
[11] T. P. A. Hase, I. Pape, D. E. Read, B. K. Tanner, H. Dürr, E. Dudzik, G. van der Laan, C. H. Marrows, and B. J. Hickey, Phys. Rev. B **61**, 15331 (2000).
[12] C. Spezzani, P. Torelli, M. Sacchi, R. Delaunay, C. F. Hague, F. Salmassi, and E. M. Gullikson, Phys. Rev. B **66**, 052408 (2002).
[13] C. Spezzani, P. Torelli, M. Sacchi, R. Delaunay, C. F. Hague, V. Cros, and F. Petroff, Appl. Phys. Lett. **81**, 3425 (2002).
[14] A. Ulyanenkov, K. Inaba, P. Mikulík, N. Darowski, K. Omote, U. Pietsch, J. Grenzer, and A. Forchel, J. Phys. D **34**, A179 (2001).
[15] M. Jergel, P. Mikulík, E. Majková, S. Luby, R. Senderák, E. Pincík, M. Brunel, P. Hudek, I. Kostic, and A. Konecníková, J. Phys. D **32**, A220 (1999).
[16] H. A. Durr, E. Dudzik, S. S. Dhesi, J. B. Goedkoop, G. van der Laan, M. Belakhovsky, C. Mocuta, A. Marty, and Y. Samson, Science **284**, 2166 (1999).
[17] K. Chesnel, M. Belakhovsky, S. Landis, J. C. Toussaint, S. P. Collins, G. van der Laan, E. Dudzik, and S. S. Dhesi, Phys. Rev. B **66**, 024435 (2002).
[18] P. Candeloro, A. Gerardino, E. Di Fabrizio, S. Cabrini, G. Giannini, L. Mastrogiacomo, M. Ciria, R. C. O'Handley, G. Gubbiotti, and G. Carlotti, Jpn. J. Appl. Phys., Part 1 **41**, 5149 (2002).
[19] A. Gerardino, E. Di Fabrizio, A. Nottola, S. Cabrini, G. Giannini, L. Mastrogiacomo, G. Gubbiotti, P. Candeloro, and G. Carlotti, Microelectron. Eng. **57-58**, 931 (2001).
[20] J. H. Underwood, E. M. Gullikson, M. Koike, P. C. Batson, P. E. Denham, and R. Steele, Rev. Sci. Instrum. **67**, 3343 (1996).
[21] K. Temst, M. J. Van Bael, V. V. Moshchalkov, and Y. Bruynseraede, J. Appl. Phys. **87**, 4216 (2000).

[22] C. Sánchez-Hanke, F. J. Castaño, Y. Hao, S. L. Hulbert, C. A. Ross, H. I. Smith, and C.-C. Kao, IEEE Trans. Magn. **39**, 3450 (2003); F. J. Castaño, Y. Hao, S. Haratani, C. A. Ross, B. Vogeli, H. I. Smith, C. Sánchez-Hanke, C. C. Kao, X. Zhu, and P. Grutter, J. Appl. Phys. **93**, 7927 (2003).

[23] The correct expression (modified Bragg law) contains also the real part of the optical index, which varies strongly across the Fe 2*p* absorption edge.

[24] Because of their position, these structures may also correspond to the so-called half-integer peaks, a sign of a superstructure of double period. Such peaks are often associated to the presence of AF order (see Ref. 17 and discussion of Fig. 9). In our case, this interpretation can be excluded on the basis of off-resonance measurements performed at 650 eV, still showing the additional structures. Our results suggest that second order contamination in the x-ray beam should be carefully checked before interpreting half order peaks as of magnetic origin.

[25] C. Spezzani, Ph.D. thesis, Université Paris-Sud, Orsay, 2003.

[26] A. Mirone, M. Sacchi, E. Dudzik, H. Dürr, G. van der Laan, A. Vaurès, and F. Petroff, J. Magn. Magn. Mater. **218**, 137 (2000).

[27] C. M. Schneider and G. Schönhense, Rep. Prog. Phys. **65**, R1785 (2002); C. M. Schneider, O. de Haas, D. Tietjen, U. Muschiol, N. Cramer, Z. Celinski, A. Oelsner, M. Klais, Ch. Ziethen, O. Schmidt, G. Schönhense, N. Zema, and S. Zennaro, J. Phys. D **35**, 2472 (2002).

[28] C. Spezzani, P. Torelli, R. Delaunay, C. F. Hague, F. Petroff, A. Scholl, E. M. Gullikson, and M. Sacchi, Physica B **345**, 153 (2004).

[29] A. Vial and D. van Labeke, Opt. Commun. **153**, 125 (1998). For recent applications, see, for instance, I. Guedes, M. Grimsditch, V. Metlushko, P. Vavassori, R. Camley, B. Ilic, P. Neuzil, and R. Kumar, Phys. Rev. B **67**, 024428 (2003).

[30] e.g., S. Landis, B. Rodmacq, and B. Dieny, Phys. Rev. B **62**, 12271 (2000); K. Matsuyama, Y. Nozaki, and T. Misumi, J. Magn. Magn. Mater. **240**, 1113 (2002).